| ARAŞTIRMA MAKALESİ | RESEARCH ARTICLE |
|---|---|

# Development of New Models Using Empirical Modeling of Global Solar Radiation and Its Application in Usak City, Turkey

## Global Güneş Radyasyonun Ampirik Modellenmesi için Yeni Modellerin Geliştirilmesi ve Uşak İlinde Uygulanması

### Rabia ERSAN[1*], Recep KÜLCÜ[2]

## Abstract

With this study, 12 empirical models in the literature, 2 new models developed within the scope of this study, SARAH and CMSAF satellite-based models, COSMO and ERA5 re-analysis solar radiation data sets in the PVGIS database were compared in order to detect the monthly average global solar radiation coming to the horizontal plane of Usak province. New models developed within the scope of the study; it uses the region's temperature, cloudiness coefficient and sunset hour angle. In comparison of the datas within the scope of the study; coefficient of determination ($R^2$), mean percent error (MPE), deviation error (MBE), root mean square error (RMSE), absolute relative error (ARE) parameters were used. As a result of the evaluations, the method that most successfully predicts the global solar radiation values of Usak province was tried to be determined. According to the monthly evaluation of the models; It was determined that 14 models and satellite-based systems have absolute relative error values below 5% in March-April-May-June, September-October and December. The most accurate estimates were realized for May in 16 of 18 different estimation methods used in the study. The coefficient of determination of empirical models and PVGIS data sets was above 0.97. When the success of the models was evaluated according to the RMSE values, It was determined that the logarithmic based Model 14 (0.90058 RMSE, 0.98327 $R^2$, -1.079894 MPE, -0.05033 MBE, 0.185628 t) which was obtained by using the sunset hour angle and the max-min temperature difference developed within the scope of this study, made the most accurate estimations. COSMO data from spatial data (1.053134 RMSE, 0.979036 $R^2$, -1.196348 MPE, -0.25105 MBE, 0.8141 t) made successful estimations, but the accuracy of the COSMO data was lower than the data estimated by Model 14. It was concluded that used the models and satellite-based systems were generally successful. As a result, In the studies to be carried out for the global solar radiation forecast of Usak province. It has been concluded that Model 14 developed within the scope of the study can be used in precise calculations and COSMO data from PVGIS datas can be used in more superficial or pre-feasibility studies.

**Keywords:** Solar energy, Global solar radiation, Modelling, PVGIS, Usak (Turkey).

[1*]**Sorumlu Yazar/Corresponding Author:** Rabia Ersan, Program of Greenhouse, Department of Plant and Animal Production, Sandıklı Vocational School, Afyon Kocatepe University, Afyonkarahisar, Turkey. E-mail: rabiaersan@aku.edu.tr ⓘD OrcID: 0000-0003-1119-4894
[2]Recep Külcü, Department of Agricultural Machinery and Technologies Engineering, Faculty of Agriculture, Isparta University of Applied Sciences, Isparta, Turkey. E-mail: recepkulcu@isparta.edu.tr ⓘD OrcID: 0000-0002-7185-6514

# Öz

Bu çalışma ile Uşak iline yatay düzleme gelen aylık ortalama global güneş radyasyonunun tespit edilebilmesi için literatürde yer alan 12 amprik model, bu çalışma kapsamında geliştirilen 2 yeni model ve PVGIS veri tabanında yer alan SARAH ve CMSAF uydu tabanlı ile COSMO ve ERA5 yeniden analiz veri setleri karşılaştırılmıştır. Çalışma kapsamında geliştirilen yeni modeller; bölgenin sıcaklık, bulutluluk oranı ve saat açısını kullanmaktadır. Çalışma kapsamındaki verilerin karşılaştırılmasında; determinasyon katsayısı (R²), ortalama yüzde hata (MPE), sapma hatası (MBE), ortalama karekök hatası (RMSE) ve yüzde hata (IeI) parametreleri kullanılmıştır. Değerlendirmeler sonucunda Uşak ilinin global güneş radyasyonu değerlerini en başarılı tahmin eden yöntem belirlenmeye çalışılmıştır. Modellerin aylık değerlendirmesine göre; Mart-Nisan-Mayıs-Haziran, Eylül-Ekim ve Aralık aylarında 14 modelin ve uydu tabanlı sistemlerin mutlak bağıl hata değerlerinin %5'in altında olduğu belirlenmiştir. Mayıs ayı için çalışmada kullanılan 18 farklı tahmin yönteminden 16'sında en doğru tahminler gerçekleşmiştir. Ampirik modellerin ve PVGIS veri setlerinin belirleme katsayısı 0,97'nin üzerindedir. Modellerin başarısı RMSE değerlerine göre değerlendirildiğinde bu çalışma kapsamında geliştirilen; saat açısı ve maks- min sıcaklık farkını kullanan logaritmik tabanlı Model 14'ün (0.90058 RMSE, 0.98327 $R^2$, -1.079894 MPE, -0.05033 MBE ve 0.185628 t) en doğru tahminleri yaptığı belirlenmiştir. Konumsal verilerden COSMO yeniden analiz verisi (1.053134 RMSE, 0.979036 $R^2$, -1.196348 MPE, -0.25105 MBE ve 0.8141 t) başarılı tahminler gerçekleştirmiş fakat COSMO verilerinin doğruluk seviyesi Model 14 tarafından tahmin edilen verilerden daha düşük gerçekleşmiştir. Çalışma ile kullanılan modellerin ve uydu tabanlı sistemlerin genel olarak başarılı olduğu sonucuna varılmıştır. Sonuç olarak Uşak ilinin global güneş radyasyonu tahmini için gerçekleştirilecek hassas hesaplamalarda çalışma kapsamında geliştirilen Model 14'ün kullanılabileceği, daha yüzeysel ya da ön fizibilite çalışmalarında PVGIS içerisinde yer alan COSMO yeniden analiz verisinin kullanılabileceği sonucuna varılmıştır.

**Anahtar Kelimeler:** Güneş enerjisi, Küresel güneş radyasyonu, Modelleme, PVGIS, Uşak (Turkey).

## 1. Introduction

The need for energy was constantly increasing due to industrialization, agricultural production and developments in urban life in the World. Fossil energy resources were used a large extent to meet the rapidly increasing energy need since the industrial revolution. However, there had been a rapid transition from fossil energy sources, which were the main source of GHGs (Greenhouse gases) that cause global climate change, to renewable resources in recent years. Solar energy was the source with the highest potential among renewable energy sources. Solar energy was a source of heat and light for our World and the living creatures on it, as well as in shaping climates. Turkey due to the geographical feature has a high solar energy potential (Artkın, 2018). The average annual sunshine duration of Turkey was calculated as 2640 hours (daily total of 7.2 hours), average total solar radiation was 1311 kWh m$^{-2}$ year$^{-1}$ (daily total of 3.6 kWh m$^{-2}$), solar energy potential was 380 billion kWh year$^{-1}$ (Anonymous, 2020a).

Önler and Kayişoğlu (2023), were determined Monthly, seasonal, and annual optimum tilt angles using meteorological insolation data from many years in the provinces of Tekirdag and Konya in the study they conducted. At optimum tilt angles, monthly, seasonal, and annual total radiation on the tilted surface were 1516.7 kWh m$^{-2}$ year$^{-1}$, 1504.1 kWh m$^{-2}$ year$^{-1}$ and 1448.1 kWh m$^{-2}$ year$^{-1}$ in Tekirdag, respectively. In Konya, these values were 1851.4 kWh m$^{-2}$ year$^{-1}$, 1833.51 kWh m$^{-2}$ year$^{-1}$ and kWh m$^{-2}$ year$^{-1}$, respectively. In both provinces, it was observed that there was no significant difference in the total radiation values coming to the tilted surface in monthly and seasonal optimum tilt angles (1%). At the annual optimum tilt angle, a decrease of approximately 5% was observed in the total amount of radiation coming to the tilted surface compared to the monthly optimum tilt angle.

As can be seen from literature studies, due to the differences in the angle of incidence of global solar radiation on the horizontal surface, the solar energy falling on the horizontal surface varies spatially, and therefore the ideal model must be determined for each location. There are many models used in global solar radiation prediction. However, these prediction models vary according to the climate and geographic characteristics of the region involved. When the prediction model determined for a region is used in a different region, the prediction model may not work. In order to gain absolute and stable results from these models, the studies should be either custommade or teste (Külcü and Ersan, 2021).

Solar radiation observations were useful data sources used to measure the average incident radiation. In the lack of solar radiation observations, it was possible to estimate the solar radiation using data obtained from nearby locations with similar climates or empirical models using parameters such as sunshine duration, cloudiness, environmental temperature and etc. (Duffie and Beckman, 1980; Kallioğlu et al., 2015). Since the repair, maintenance and investment costs of solar radiation measuring devices are very high, they cannot be placed at every measurement point. For this reason, empirical models or satellite-based forecasting systems are usually used in solar radiation calculations (Işık and İnallı, 2011; Gül and Çelik, 2017).

Psiloglue et al. (2020), examined the performance of the estimated solar radiation components obtained via the Meteorological Radiation Model, satellite-based data sets (CAMS, PVGIS-CMSAF-SARAH) and reanalysis (PVGIS-ERA5) against ground measurements taken with the Sunshine-Pyranometer at Methoni Station, Greece. Then, they compared the estimation results obtained. The MRM uses astronomical values (solar constant, seasonally adjusted Sun-earth distance, solar altitude and azimuth, inclination) and widely available meteorological parameters (air temperature, relative humidity, surface pressure and sunshine fraction) as inputs. The results showed that MRM simulates the global (RMSE~12%) and direct horizontal (RMSE~16-21%) irradiations in higher accuracy compared to CAMS (RMSE ~19-28%, respectively), while CAMS represented better the diffuse radiation (RMSE 46% for MRM and RMSE 38% for CAMS). The PVGIS data sets revealed high uncertainties in the simulation of the instantaneous solar irradiances; their performance was lower compared to MRM and CAMS, although a direct comparison cannot be applied. CMSAF showed better estimates, while the reanalysis ERA5 resulted in similar statistics with the satellite-based SARAH.

Supit and Van Kappel (1998) aimed to use daily global radiation estimates as input for the European Union Plant Growth Monitoring System. For this purpose, they developed an estimation model from the maximum-minimum temperature and average daily cloudiness datas obtained from meteorological sources. The developed model had been tested in various regions of Europe from Finland to Italy. Comparison of measured and estimated

global irradiance values in the tested regions was made, and an average of 2.48 RMSE and -0.25 MJ m$^{-2}$ day MBE values were found.

Almorox et al. (2013) in the daily global solar radiation estimation study from the temperature data of Canada de Luque, Cordoba, Argentina region; they made estimations of solar radiation with Hargreaves-Samani, Allen, Samani, Bristow-Campbell, Almorox and linear regression models. The results showed that, all the analyzed models were robust and accurate (R$^2$ and RMSE values between 0.87 to 0.89 and 2.05 to 2.14, respectively), so global radiation can be estimated properly with easily available meteorological variables when only temperature data are available. While Hargreaves-Samani, Allen, and Bristow-Campbell models can be used with typical values to estimate solar radiation, Samani and Almorox models have been suggested to be used after their coefficients are calibrated for the region in which they will be used by concluding that only Model 3 has a significant improvement (0.887 R$^2$) for its local applicability.

Kulcu et al. (2017) made estimation a monthly average daily global solar radiation using 6 empirical models in Mersin province, Turkey. Model 6 in Equation 1 where -hour angle and cloudiness coefficient were used and found as the most successful estimation model for Mersin province with 0.8576 RMSE, -0.3251 MBE, -4.7622 MPE values, respectively.

$$\frac{H}{H_0} = \left[\frac{1.333962\left(\frac{S}{S_0}\right)}{0.044188\,w_s}\right] + 0.002578\,w_s \tag{Eq. 1}$$

In this study; the data of Usak (Turkey) meteorology station, the solar energy estimation models developed by other researchers and developed in this study, the solar radiation data obtained using forecasts with the SARAH and CMSAF satellite-based and the re-analysis data sets of COSMO and ERA5 in PVGIS were compared. The ideal global solar radiation estimation model has been determined for the city of Usak, Turkey.

## 2. Materials and Methods

Solar energy calculations on the horizontal surface within the scope of the study; 35S 653505 -36S 241430 longitude, 4228190-4311902 (UTM grid system) and 907 m elevation was carried out for the provincial borders of Usak province (*Figure 1*). Usak Province is located in the Central Western Anatolia part of the Aegean region, Afyonkarahisar in the east, Manisa in the west, Kutahya in the north and Denizli in the south. The area of the province is 534.063 hectares and it has 6 districts. The region generally consists of mountainous and rugged lands. It looks like wavy plateaus split by a dense network of valleys. In places, mountains rise above the plateau plains. Murat Mountain, the most important of these mountains and also the highest point of Innerwest Anatolia, has an altitude of 2309 meters. 57.5% of the provincial lands consist of plateaus, 37% of mountains and 5.5% of plains. Murat, Bulkaz and Ahır Mountains form the natural borders of the province in the north, northeast and east. The west of the provincial lands opens to the Aegean Region with the Gediz valley. The provincial lands look like wavy plateaus split by many valleys. These plateaus descend from northeast to southwest and take a slightly wavy appearance in some parts. The province of Usak is geographically located between the Aegean and the Central Anatolia region. As a natural result of this location, transition climate characters prevail in Usak province (Anonymous, 2020b). In *Table 1*, the average climate data of Usak for many years (1939-2020) were presented. The average monthly total precipitation amount was 557.6 mm, the average temperature was 12.5 °C, the average lowest temperature was 6.8 °C, and the average maximum temperature was 18.5 °C (Anonymous, 2020c). The annual radiation amount is in the range of 1550-1650 kWh m$^{-2}$ year. On province basis, the average incoming solar radiation in Turkey 1350 kWh m$^{-2}$ years. Considering this situation, Usak province is one of the suitable conditions to invest in solar energy (Anonymous, 2020a).

### Table 1. Climate data of Usak for long years (1939-2020) (Anonymous, 2020c)

| | January | February | March | April | May | June | July | August | September | October | November | December | Annual |
|---|---|---|---|---|---|---|---|---|---|---|---|---|---|
| Average temperature (°C) | 2.3 | 3.3 | 6.2 | 10.9 | 15.6 | 19.9 | 23.4 | 23.4 | 19.1 | 13.7 | 8.3 | 4.2 | 12.5 |
| Average High Temperature (°C) | 6.8 | 8.3 | 11.8 | 16.8 | 21.8 | 26.5 | 30.3 | 30.5 | 26.3 | 20.3 | 14.1 | 8.8 | 18.5 |
| Average Lowest Temperature (°C) | -1.3 | -0.6 | 1.4 | 5.2 | 9.2 | 12.6 | 15.5 | 15.6 | 11.9 | 7.9 | 3.8 | 0.7 | 6.8 |
| Average Sunshine duration (hour) | 3.9 | 4.6 | 5.5 | 6.8 | 8.8 | 10.9 | 11.8 | 11.3 | 9.7 | 7.3 | 5.3 | 3.8 | 7.5 |
| Average Rainy Days | 12.2 | 10.7 | 10.8 | 11.0 | 10.1 | 6.0 | 3.1 | 2.4 | 3.4 | 7.1 | 8.5 | 12.7 | 98.0 |
| Average Monthly Total Rainfall (mm) | 73.4 | 66.7 | 58.0 | 50.9 | 48.0 | 27.2 | 16.5 | 12.6 | 18.6 | 42.2 | 58.9 | 84.6 | 557.6 |
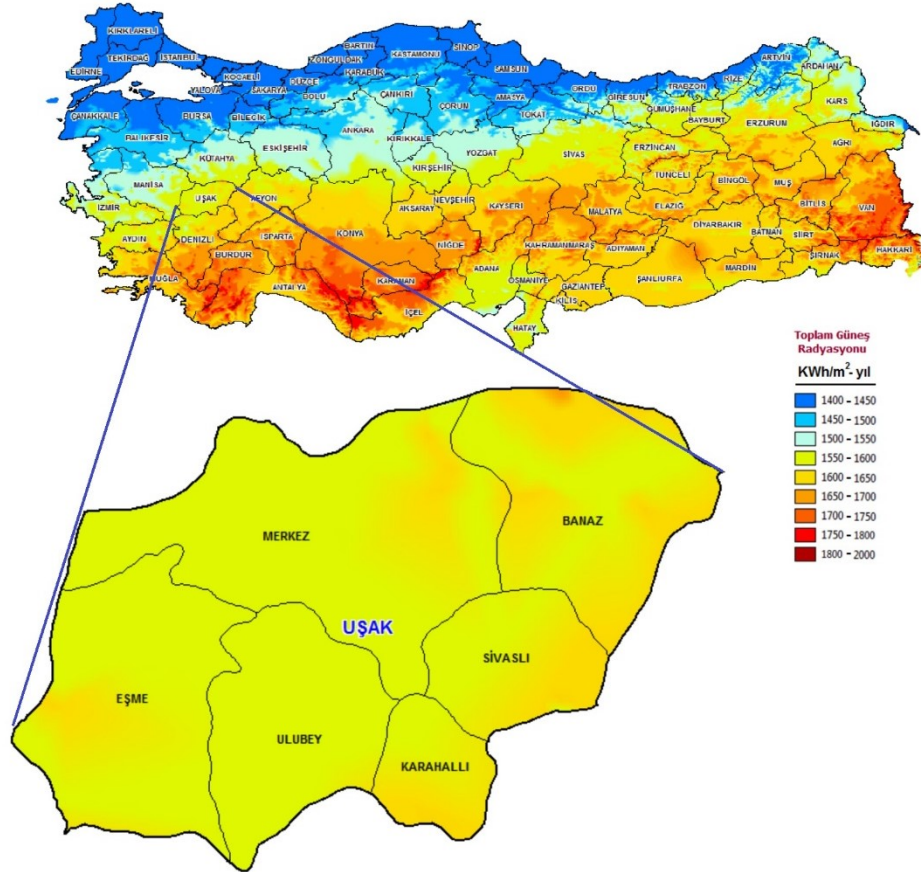
**Figure 1. Solar energy potential and location map of Usak province (Anonymous, 2021a)**

### 2.1. Calculation of the amount of solar radiation coming out of the atmosphere in Usak province

The amount of extra-terrestrial radiation coming on a horizontal surface in a day was calculated using Equation 2 (Duffie and Beckman, 1980);

$$H_O = \frac{24 x 3600 x G_{SC}}{\pi}\left[1 + 0.033\left(Cos\frac{360n}{365}\right)\right] * \left[Cos\varphi\ Cos\delta\ sinw_s + \frac{\pi}{180}w_s Sin\varphi Sin\delta\right] \qquad \text{(Eq.2)}$$

The declination angle refers to the angle between the plane around which the earth rotates around the sun at noon (when the sun is on the local meridian) and the equatorial axis. This angle takes maximum value on June 21st and minimum value on December 21st, and it becomes zero on the 21st of March and 21st of September. The declination angle was calculated using Equation 3. *Table 2* was used to find the value of n (Cooper, 1969; Duffie and Beckman, 1980).

$$\delta = 23.45\ Sin\left(360\frac{n+284}{365}\right) \qquad \text{(Eq.3)}$$

Sunset hour angle (w_s) expresses the angle between the latitude where the sunlight (at the time the sunset) and the latitude calculated using equation numbered 4 (Duffie and Beckman, 1980);

$$w_s = arccos[-tan(\varphi)tan(\delta)] \qquad \text{(Eq.4)}$$

S used in the models indicates the sunshine duration of that day on the date and coordinate calculated, and $S_0$ indicates the total day length in the same day and in the same place. While the S value was determined according to meteorological measurements, the S0 value was calculated using the equation numbered 5 (Duffie and Beckman, 1980);

$$S_{0=}\frac{2}{15}\cos^{-1}[-\tan(\varphi)\tan(\delta)] \qquad \text{(Eq.5)}$$

**Table 2. Recommended Average Days for Months and Values of n by Months (Klein, 1977; Duffie and Beckman, 1980)**

| Month | $n$ for $i$th day of month | For Average Day of Month | | |
|---|---|---|---|---|
| | | Date | $n$ | $\delta$ |
| January | $i$ | 17 | 17 | -20.9 |
| February | $31 + i$ | 16 | 47 | -13.0 |
| March | $59 + i$ | 16 | 75 | -2.4 |
| April | $90 + i$ | 15 | 105 | 9.4 |
| May | $120 + i$ | 15 | 135 | 18.8 |
| June | $151 + i$ | 11 | 162 | 23.1 |
| July | $181 + i$ | 17 | 198 | 21.2 |
| August | $212 + i$ | 16 | 228 | 13.5 |
| September | $243 + i$ | 15 | 258 | 2.2 |
| October | $273 + i$ | 15 | 288 | -9.6 |
| November | $304 + i$ | 14 | 318 | -18.9 |
| December | $334 + i$ | 10 | 344 | -23.0 |

*Do not use for $|\varphi| > 66.5^o$.*

### 2.2.Empirical estimation models used in the study

In the modeling of solar radiation reaching Usak, Equation 6-17 in the literature and Equation 18-19 developed within the scope of this study were used.

Model 1 [Angstrom-Prescott model]; In order to obtain maximum benefit from solar energy and to determine its efficiency, it is extremely important to simultaneously obtain solar radiation and sunshine duration at the same point. To show this relationship, first Kimball (1919) and then Angstrom (1924) developed equations. Later, Prescott (1940) has developed the Angstrom equation by dimensionlessing it with extraterrestrial solar radiation and insolation time. And the model in Equation 6 has been called Angstrom-Prescott since 1940 (Güçlü, 2019). The Angstrom-Prescott model is one of the most widely used estimation methods for calculating monthly average daily irradiance.

$$\frac{H}{H_0} = c_1 + c_2 \left( \frac{S}{S_0} \right) \tag{Eq.6}$$

Model 2 (Elagib and Mansell, 2000);

$$\frac{H}{H_0} = c_1 + c_2 \left( \frac{S}{S_0} \right)^{c_3} \tag{Eq.7}$$

Model 3 (El-Metwally, 2005);

$$\frac{H}{H_0} = c_1^{(1/S)} \tag{Eq.8}$$

Model 4 (Külcü, 2015);

$$\frac{H}{H_0} = \left[ \frac{c_1 \left( \frac{S}{S_0} \right)}{c_2 \, w_s} \right] + c_3 w_s \tag{Eq.9}$$

Model 5 (Bahel et al., 1987);

$$\frac{H}{H_0} = c_1 + c_2 \left( \frac{S}{S_0} \right) + c_3 \left( \frac{S}{S_0} \right)^2 + c_4 \left( \frac{S}{S_0} \right)^3 \tag{Eq.10}$$

Model 6 (Ampratwum and Dorvlo, 1999);

$$\frac{H}{H_0} = c_1 + c_2 \left( \frac{S}{S_0} \right) + c_3 log \left( \frac{S}{S_0} \right) \tag{Eq.11}$$

Model 7 (Almorox and Hontoria, 2004);

$$\frac{H}{H_0} = c_1 + c_2 exp \left( \frac{S}{S_0} \right) \tag{Eq.12}$$

Model 8 (Dogniaux and Lemoine, 1983); Unlike other models, latitude degree was used in this model.

$$\frac{H}{H_0} = c_1 + \left[ c_2 \left( \frac{S}{S_0} \right) + c_3 \right] \varphi + c_3 \left( \frac{S}{S_0} \right) \tag{Eq.13}$$

Model 9 (Külcü, 2019); In this model, unlike other models, solar radiation was estimated by using the logarithmic

relationship of the cloudiness coefficient with the hour angle.

$$\frac{H}{H_0} = c_1 + c_2 log\left(\frac{S}{S_0}\middle/w_s\right) + c_3 \left(\frac{S}{S_0}\right) \tag{Eq.14}$$

Model 10 (Hargreaves et al., 1985); Unlike previous models, maximum and minimum temperature differences was used in Model 10.

$$\frac{H}{H_0} = c_1 * (\Delta T)^{0.5} + c_2 \tag{Eq.15}$$

Model 11 (Chen Model (Coppolino, 1994));

$$\frac{H}{H_0} = c_1 * ln(\Delta T) + c_2 \tag{Eq.16}$$

Model 12 (Bristow and Campbell, 1984);

$$\frac{H}{H_0} = c_1 * [1 - \exp\{-c_2 * (\Delta T)^{c_3}\}] \tag{Eq.17}$$

Model 13; In this study, it was a new model developed using the linear logarithmic method. There were various solar radiation estimation models based on $S/S_o$ ratio, including linear, second order, third order and logarithmic. In this model, the cloudiness coefficient was fixed with the $c_2$ coefficient and its logarithm was taken. Also, the maximum-minimum temperature changes were fixed with the $c_3$ coefficient and the last coefficient was summed up with the $c_4$ coefficient and a linear relationship is established with the radiation coming from the extraterrestrial. And thus, the global monthly average daily solar radiation amount was estimated from here;

$$H/H_0 = c_1 * log[(c_2 * S/S_0) + (c_3 * \Delta T)] + c_4 \tag{Eq.18}$$

Model 14; An second liner logarithmic model developed within the scope of this study. In this model, the effects of temperature changes and temporal dependence had been demonstrated in calculation of the global monthly average daily solar radiation by using the hour angle instead of the cloudiness coefficient;

$$H/H_0 = c_1 * log[(c_2 * w_s) + (c_3 * \Delta T)] + c_4 \tag{Eq.19}$$

### 2.3. PVGIS-based data sets used within the scope of the study

With Remote Sensing (RS) technologies, it is fast and easy to collect data belonging to a large part of our World. RS technologies are also using among the basic data sources of renewable energy sources as they are in many fields today. Data provided by RS technologies or meteorological measurements are collected in GIS-based software. And thanks to the calculation modules included in this software, the solar radiation estimation of the desired location can be made hourly, daily, monthly and yearly. Photovoltaic Geographical Information System (PVGIS) is one of the web-based versions of these software. It was created by the European Commission and offered for open access in a web browser. Energy production data was calculated using different satellite bases and parameters with PVGIS positional solar radiation and photovoltaic systems. These variables offer different success in different positions (Anonymous 2021b).

In the study, monthly solar radiation data obtained by using SARAH and CMSAF satellite-based (COSMO and ERA5) data sets in kWh m$^{-2}$ unit of Usak province were obtained from the PVGIS web portal (*Table 3*). These data were converted to MJ m$^{-2}$ and monthly average daily solar radiation values were obtained proportioning the days of each month.

*Table 3. Properties of solar radiation databases in PVGIS (Anonymous, 2021b)*

| Database | Type | Start Year | End Year | Spatial Resolution |
|----------|------|-----------|----------|--------------------|
| PVGIS-SARAH | Satellite | 2005 | 2016 | 0.05° x 0.05° (~ 5 km) |
| PVGIS-CMSAF | Satellite | 2007 | 2016 | 0.025° x 0.025° (~ 2.5 km) |
| PVGIS-ERA5 | Re-analysis | 2005 | 2016 | 0.25° x 0.25° (~ 25 km) |
| PVGIS-COSMO | Re-analysis | 2005 | 2015 | 0.055° x 0.055° (~ 5 km) |

*2.4. Statistical parameters used to test the estimation success of the models*

The estimation capabilities of the models examined within the scope of the study were compared. Monthly average data were compared using parameters MPE (mean percentage error) in Equation 20, MBE (mean bias error) in Equation 21, RMSE (root mean square error) in Equation 22, $R^2$ (determination coefficient) in Equation 23. And, monthly data were compared using the (ARE) (absolute relative error) parameter in Equation 24.

The $R^2$ is an indicator of the inter-variable dependence, and its close to one indicates that there is a strong bond between the variables. The RMSE is an indicator of the deviation between the measured and calculated values and provides information about the short-term performance of the model under study. The closer the RMSE value is to zero, the better the performance of the model is evaluated. MBE provides information about the long-term performance of the model under study. The closer the MBE value is to zero, the higher the performance of the model. If this value is positive, it indicates that an estimate has been made above the calculated value, if it is negative, it indicates that an estimation has been made below the calculated value. The MPE is the indicator of the percentage value of the deviation between the measured and calculated values, and the closer the value to zero, the higher the performance of the model (Tırmıkçı, 2018). The ratio of the absolute error to the measured value gives the relative error. Relative error is a type of error that shows proportionally how close to the real value is. In most studies, relative error means more than absolute error (Anonymous, 2021c). Relative errors between -10% and +10% are acceptable value ranges (Skeiker, 2006). An useful measure of goodness is absolute relative error (Dyer and Dyer, 2007). Absolute relative error is calculated by proportioning the absolute error to the measured value and taking the percentage (Navarro, 1992; Green and Tashman, 2009). Absolute relative error getting too close to zero means that the estimate is very close to the target value (Anacan et al., 2018; Marfo and Okyere, 2019).

$$MPE = \frac{1}{N}\sum_{i=1}^{N}\left(\frac{H_{ip}-H_{io}}{H_{io}}\right)x100 \qquad (Eq.20)$$

$$MBE = \frac{1}{N}\sum_{i=1}^{N}\left(H_{ip}-H_{io}\right) \qquad (Eq.21)$$

$$RMSE = \sqrt{\frac{1}{N}\sum_{i=1}^{N}\left(H_{ip}-H_{io}\right)^2} \qquad (Eq.22)$$

$$R^2 = \frac{\sum_{i=1}^{N}(H_{ip}-H_{ipa})(H_{io}-H_{ioa})}{\sqrt{[\sum_{i=1}^{N}(H_{ip}-H_{ipa})^2][\sum_{i=1}^{N}(H_{io}-H_{ioa})^2]}} \qquad (Eq.23)$$

$$ARE = \left(I\frac{H_{ip}-H_{io}}{H_{io}}I\right)x100 \qquad (Eq.24)$$

### 3. Results and Discussion

*3.1. Global Solar Radiation Data of Usak Province*

According to the radiation values measured in Usak, the lowest global solar radiation reaches the ground surface in December (6.83 MJ m$^{-2}$ day$^{-1}$) and the highest radiation in July (26.83 MJ m$^{-2}$ day$^{-1}$). Global solar radiation values of Usak province according to meteorological data varies between 6.83-7.67 MJ m$^{-2}$ day$^{-1}$ in December-January, 8.14-8.98 MJ m$^{-2}$ day$^{-1}$ in November-February, 12.88-13.05 MJ m$^{-2}$ day$^{-1}$ in October-March, 18.14-18.29 MJ m$^{-2}$ day$^{-1}$ in September-April, 20.87-22.81 MJ m$^{-2}$ day$^{-1}$ in August-May and 25.53-26.83 MJ m$^{-2}$ day$^{-1}$ in June-July. It was seen that the estimation models and PVGIS-based data sets used within the scope of this study generally reveal estimates close to the measured data.

*3.2. Global Solar Radiation Estimate Models and PVGIS Based Datasets*

The global solar radiation values estimated by the models used within the scope of this study, the global radiation values based on PVGIS and the changes of the global radiation values measured from the Usak Meteorology Station were given in *Table 4* using the color scale. According to the color scale, Model 3, 4, ERA5 and SARAH made quite different estimates from the measured data. Deviations of other models and data sets were at lower levels. In *Table 5*, the comparison of each of the models with the measured monthly average daily solar irradiance data was given as graphic template and interpreted.

***Table 4. Measured and estimated radiation information table of Usak province***

| H (MJ m⁻² day⁻¹) | 17 January | 16 February | 16 March | 15 April | 15 May | 11 June | 17 July | 16 August | 15 September | 15 October | 14 November | 10 December |
|---|---|---|---|---|---|---|---|---|---|---|---|---|
| Measured | | | | | | | | | | | | |
| Model 1 | | | | | | | | | | | | |
| Model 2 | | | | | | | | | | | | |
| Model 3 | | | | | | | | | | | | |
| Model 4 | | | | | | | | | | | | |
| Model 5 | | | | | | | | | | | | |
| Model 6 | | | | | | | | | | | | |
| Model 7 | | | | | | | | | | | | |
| Model 8 | | | | | | | | | | | | |
| Model 9 | | | | | | | | | | | | |
| Model 10 | | | | | | | | | | | | |
| Model 11 | | | | | | | | | | | | |
| Model 12 | | | | | | | | | | | | |
| Model 13 | | | | | | | | | | | | |
| Model 14 | | | | | | | | | | | | |
| COSMO | | | | | | | | | | | | |
| ERA5 | | | | | | | | | | | | |
| SARAH | | | | | | | | | | | | |
| CMSAF | | | | | | | | | | | | |

| Color Scale | | | | | | | | | | | |
|---|---|---|---|---|---|---|---|---|---|---|---|
| 4-5 | 5-6 | 6-7 | 7-8 | 8-9 | 9-10 | 10-11 | 11-12 | 12-13 | 13-14 | 14-15 | 15-16 |
| 16-17 | 17-18 | 18-19 | 19-20 | 20-21 | 21-22 | 22-23 | 23-24 | 24-25 | 25-26 | 26-27 | 27-28 |
| 28-29 | | | | | | | | | | | |

In Model 1, it was observed that the estimates were higher than the measured values between February-March, early August, mid-September, and late October-November. And the opposite situation was observed in the period from mid-April to the end of July, and the estimates were below the measured values. The estimates were realized as expected in the period from end of March to mid-April, end of July, mid-September-end of October and in December. Estimates close to Model 1 were obtained from Model 2. This is because the Equation structures of the two models are similar to each other. During the period from the end of April to mid-May, and the period from mid-September to mid-October, the estimates obtained with Model 3 approached the measured values and made high estimates in this period. It was observed that the estimations were higher than the measured values in the summer months, and the estimations were realized below the measured values in the winter and spring months. The fact that this model is based on the sunshine duration has been effective in estimating high irradiance values in the summer months and low irradiance values in the winter months.

The estimates obtained by Model 4 were high for the first 6 months of the year, while the last 6 months made low estimates. It gave results close to the values measured in January, June and August. Estimates close to Models 1 and 2 were obtained from Model 5. Model 6 was a model based on the logarithm of the cloudiness coefficient developed by Ampratwum and Dorvlo (1999). This model made estimates close to the measured values in January, the period from the end of March to May, in July, the period from mid-September to November and in December. It was observed that the estimates moved away from the measured values in the June-August period. Model 7 made estimates close to the measured values in January, from late March to mid-April, in late July, from mid-September to October, and in December. The most distant estimates were observed in February and August. Model 8 made estimates close to the values measured in January, end of March, mid-April, end of July, mid-October and December. The most distant estimates were in February and August. Model 9 had quite accurately estimated values for January, end of March, mid-April, end of July, the period from mid-September to the end of October and in December. It made the most distant estimations in February and August. Model 9 made estimates very close to Model 8.

***Table 5. Comparison graphs of monthly average daily solar radiation data estimated and measured by models***

| Model 1 | Model 2 |
| --- | --- |
|  |  |
| Model 3 | Model 4 |
|  |  |
| Model 5 | Model 6 |
|  |  |
| Model 7 | Model 8 |
|  |  |

*Table 5. (contiuned) Comparison graphs of monthly average daily solar radiation data estimated and measured by models*
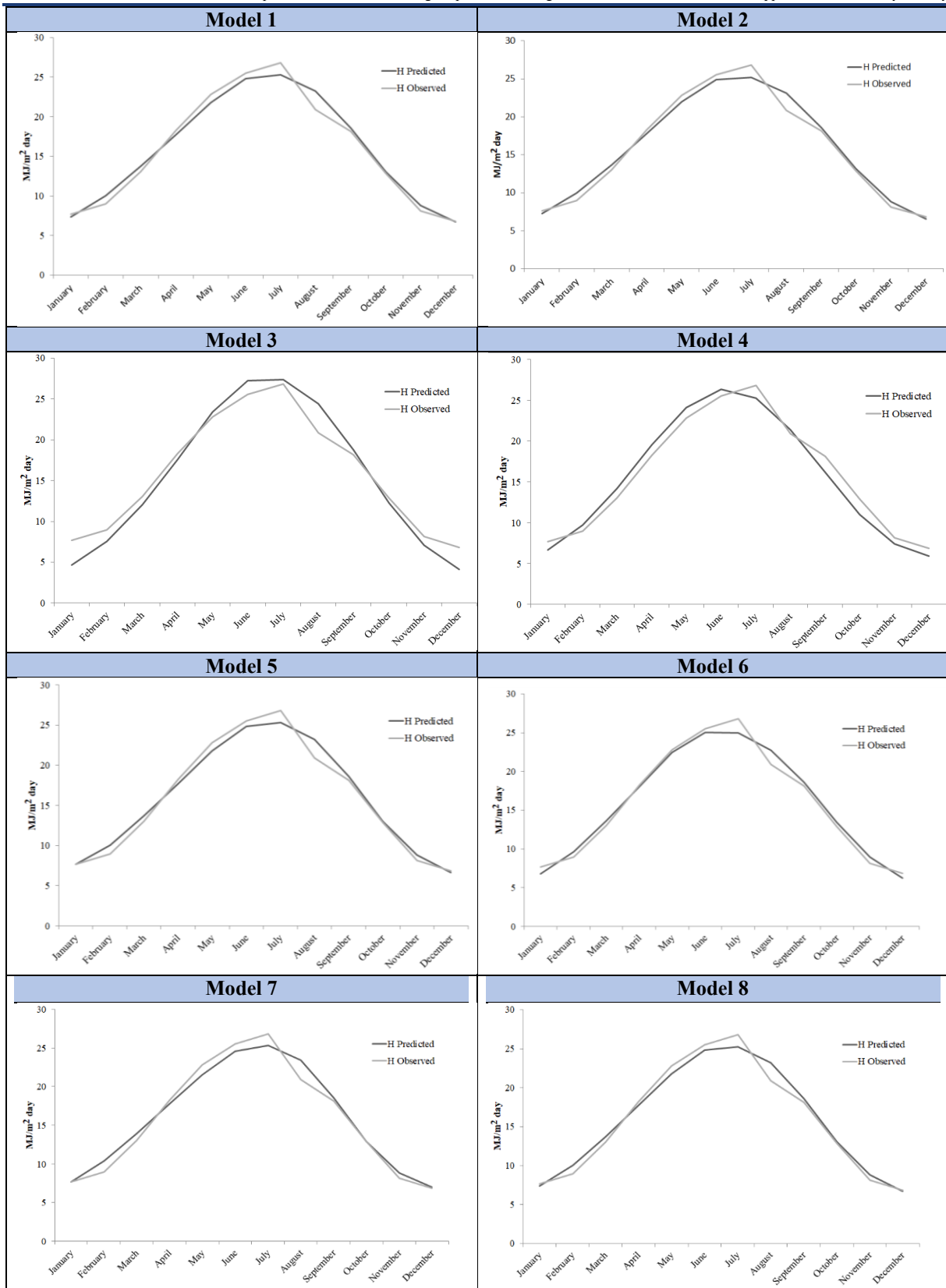
| Model 9 | Model 10 |
|---|---|



| Model 11 | Model 12 |
|---|---|



| Model 13 | Model 14 |
|---|---|
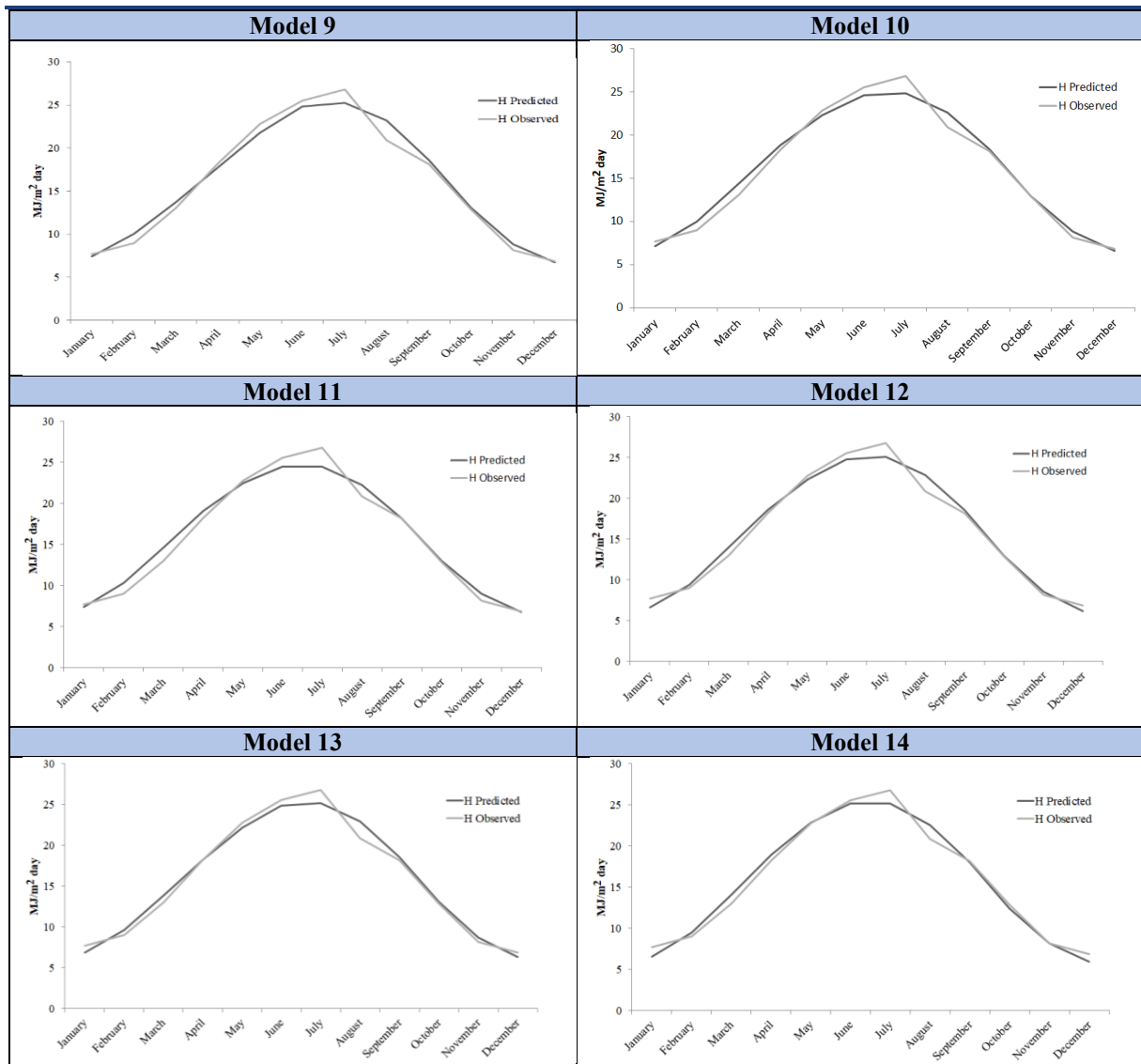


While Model 10 makes estimates close to the values measured in January, the period from mid-April to mid-May, late July, mid-October and December, the most distant estimates were realized in February and March. Model 11 made estimates close to the values measured during the period in January, the period end of April until mid-May, in early August, the period from first week of September to the last week of October and in December. The estimates from January to April were observed above the measured values and below the measured values between May and July. The furthest estimate came in July. Model 12 had produced estimates close to the values measured in the period February, from to mid-April to mid-May, in early August and from mid-September to December. The estimates were above the measured values between February-April and August-September, and below the values between May-July. The furthest estimate came in July. Model 13 obtained estimates close to the measured values in early February, in April, in early August and from mid-September to December. The estimates were above the measured values between February-April and August-September, and below the values between May-July. The furthest estimate came in July. Model 14 made estimates close to the values measured in early February, April, early August and from mid-September to December. The estimates were above the measured values between February-April and August-September, and below the values between May-July. The furthest estimate came in July. Especially in the late spring-beginning of summer and autumn period, estimates close to the measurements were obtained.

In recent years, solar radiation estimations can be made by comparing and evaluating land measurements with satellite and re-analysis datas as well as empirical models (Ineichen, 2014; Urraca et al., 2017, 2018; Feng et al., 2019). *Figure 2* shows the data obtained by using SARAH and CMSAF satellite-based and COSMO and ERA5 re-analysis global solar radiation estimate data sets for Usak province.

When the global solar radiation values obtained with the COSMO re-analysis data were examined, it was seen that estimates were made close to the monthly average daily radiation data measured in January, April, July, September and November. Estimates were obtained above the measured values between January-April and August-September, and below the measured values between April-August and September-November. The furthest estimate came in July. When the data obtained with the ERA 5 re-analysis data are examined, it was seen that estimates were obtained above the monthly average daily radiation data measured in all months of the year. The closest estimates were made in January, May-July, September-October and December. When the radiation graph obtained with SARAH satellite data was examined, it was seen that estimates were obtained above the monthly average daily radiation data measured in all months of the year. The closest estimates were made in January, May, September-October and December. The most distant estimates were observed in the months of July-August. When the radiation graph obtained with CMSAF satellite data was examined, it had been observed that estimates above the monthly average daily radiation data measured in all months of the year, and it had been observed that estimates close to the radiation data obtained from SARAH satellite data.
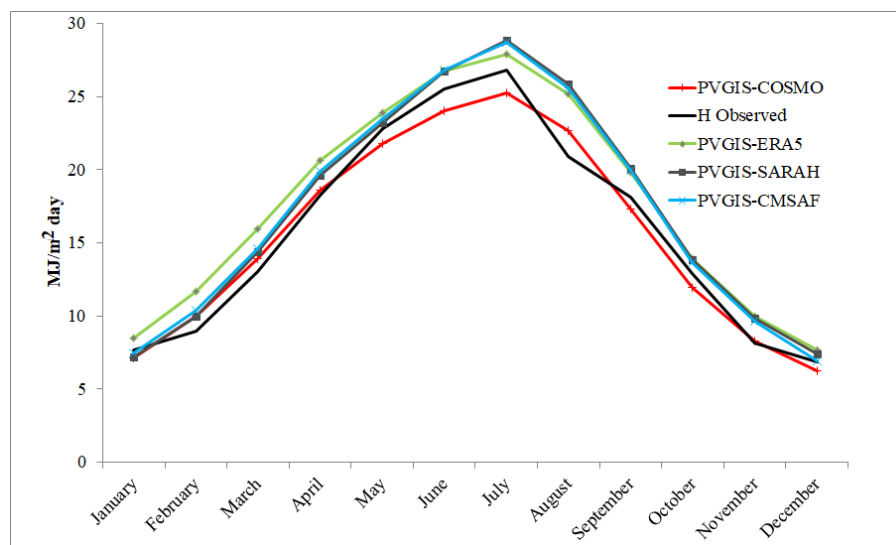


***Figure. 2. Comparison graphs of the daily radiation data measured, the radiation data obtained by re-analysis and the satellites in the PVGIS database***

When the estimated values obtained by the satellite data and re-analysis with the radiation measurements coming to the horizontal surface were evaluated together; It had been observed that the radiation estimates obtained with satellite-based data were higher than the measured values. As a matter of fact, Frank et al. (2018) reported that re-analysis data overestimated the radiation incident on the global horizontal surface in cloudy conditions. In a similar study, Psiloglue et al. (2020) reported that while satellite data and ground measurement radiation data obtained in cloudless weather conditions were in harmony with each other, they showed high uncertainty in cloudy or partially cloudy weather conditions.

The monthly success of the models and satellite-based estimation data used within the scope of the study were interpreted according to the IeI values in *Table 6*. In January, absolute relative errors were obtained below 1% from Model 5 and Model 7, 3% from CMSAF satellite data, and 3-4% from Model 11, Model 9, Model 1 and Model 8. An absolute relative error of 5% was obtained from Model 12 in February. The absolute relative error of other estimation models did not follow this level in February and was realized in the range of 5.6-29.8%. In March, an absolute relative error in the range of 4-5% was obtained from Model 6, Model 5 and Model 2. In April, absolute relative errors were obtained in the range 0.3% from Model 13, 1-2% from Model 6, COSMO re-analysis satellite data and Model 12, 2-3% from Model 2, Model 7, Model 9, Model 1, Model 8 and Model 10, 3-4% from Model 5 and Model 14, 4-5% from Model 3 and Model 11. It was observed that 14 out of 18 estimation sets used in April had an absolute relative error below 5% and in the other 4 estimation sets between 5-12.7%. While an absolute relative error of less than 5% was obtained from 16 of the 18 estimation data sets used in May, an absolute relative error of 5.7% was obtained from Models 7 and Model 4. When the forecasts obtained with the estimation models used in the study and satellite-based data sets are evaluated, the most successful estimations during the year were obtained in May. In June, while the estimates obtained from CMSAF satellite data, COSMO re-analysis data and Model 3 equation, respectively, 5.1%, 6.0% and 6.7% absolute relative errors were obtained, below 5% absolute

relative errors were obtained from other estimation sets. In July, it was obtained an absolute relative error below 5% from Model 3 and ERA5 re-analysis estimation set, and was obtained below 8.7% from other estimation sets. In August, an absolute relative error below 5% was obtained from the Model 4 estimation model, and an absolute relative error between 5-23.8% was obtained in other estimation sets. In September, the absolute relative error was obtained in the range of less than 1% from Model 11 and Model 14, 1-2% from Model 10 and Model 7, 2-3% from Model 12, Model 6, Model 13, Model 9, Model 1, Model 8, Model 2 and Model 5, 3.5% from Model 3. Also, from the satellite data sets, an absolute relative error of 4.7% was obtained from the COSMO re-analysis data. In October, an absolute relative error below 1% from Model 7, Model 12 and Model 10, between 1-2% from Model 11, Model5, Model 8, Model 1, Model 9, Model 13 and Model 2, 3.6% from Model 14, 4.2% from Model 6 was obtained. The absolute relative error of other data sets was between 5.1-14.4%. In November, an absolute relative error was obtained 0.8% from the Model 14, %1.4 from the COSMO re-analysis data, %5.3-22.2 from the other estimation sets. In December, Model 11 with a value of 0.2%, CMSAF satellite data, Model 9, Model 1 and Model 8 between 1-2%, Model 5 and Model 7 2-3%, Model 2 and Model 10 3-4% with an absolute relative error made successful estimations close to the measured value. In this month, estimates far from the measured value were obtained with a value of 39.9% from the Model 3 estimation model. The absolute relative error in the range of 7.7-13.9% was obtained from other estimation models and data sets.

According to the monthly evaluation error analysis results of estimate models and PVGIS satellite data sets, the most successful estimations were obtained in April-June, September-October and December (below 5%). An error of less than 39.9% was obtained from all estimation models and satellite-based datasets. With these values, very reasonable estimates that were close to reality had been obtained.

The monthly average of the absolute relative errors of the monthly average daily global solar radiation data of the COSMO, ERA5, SARAH and CMSAF data sets in *Table 6* were 6.1%, 13.4%, 10.0% and 9.3%, respectively. The RMSE values of these data sets were 1.053134, 2.077154, 1.893419 and 1.840986, respectively (*Table 7*). When the PVGIS data sets were compared within themselves, values close to the real values were obtained with the order of COSMO> CMSAF> SARAH> ERA5, as can be seen from the RMSE and absolute relative error values.

Models 13 and 14 were the models developed within the scope of this study. It had been seen that these two models were among the top 4 most successful models. As a result of evaluating the estimation success of the models, it took place Model 14 ranks first with 0.90058 RMSE and 0.98327 $R^2$ value, Model 6 second with 0.92664 RMSE, 0.98226 $R^2$ value, Model 13 third with 0.93959 RMSE, 0.98166 $R^2$ value, Model 12 fourth with 0.952089 RMSE, 0.980939 $R^2$ value in the first four of the 18 models used.

Within the scope of the study, when the satellite-based data sets and models used to estimation the global solar radiation of Usak were evaluated together, it was seen that the most successful estimations were made by Model 14 developed within the scope of this study (0.90058 RMSE, 0.98327 $R^2$). This model was followed by Model 6 (0.92664 RMSE, 0.981226 $R^2$) developed by Ampratwum and Dorvlo (1999) and Model 13 (0.939589 RMSE, 0.98166 $R^2$) developed within the scope of this study, respectively. The estimation success of satellite-based data sets was lower than the models.

### Table 6. The success ranking of the models according to the percentege absolute relative error (ARE%) values

| January | | February | | March | | April | | May | | June | | July | | August | | September | | October | | November | | December | |
|---|---|---|---|---|---|---|---|---|---|---|---|---|---|---|---|---|---|---|---|---|---|---|---|
| Model 5 | 0.0 | Model 12 | 5.0 | Model 6 | 4.5 | Model 13 | 0.3 | Model 14 | 0.2 | Model 14 | 1.3 | Model 3 | 2.0 | Model 4 | 2.4 | Model 11 | 0.2 | Model 7 | 0.0 | Model 14 | 0.8 | Model 11 | 0.2 |
| Model 7 | 0.2 | Model 14 | 5.6 | Model 5 | 4.8 | Model 6 | 1.3 | Model 6 | 1.5 | Model 6 | 1.8 | ERA5 | 4.1 | Model 11 | 6.6 | Model 14 | 0.9 | Model 12 | 0.2 | COSMO | 1.4 | CMSAF | 1.1 |
| CMSAF | 3.0 | Model 6 | 7.5 | Model 2 | 5.0 | COSMO | 1.6 | Model 11 | 1.5 | Model 2 | 2.6 | Model 7 | 5.7 | Model 14 | 8.0 | Model 10 | 1.2 | Model 10 | 0.4 | Model 12 | 5.3 | Model 9 | 1.6 |
| Model 11 | 3.5 | Model 13 | 7.5 | Model 8 | 5.2 | Model 12 | 2.0 | SARAH | 1.7 | Model 13 | 2.6 | Model 5 | 5.7 | Model 10 | 8.3 | Model 7 | 2.0 | Model 11 | 1.1 | Model 13 | 7.4 | Model 1 | 1.6 |
| Model 9 | 3.8 | Model 4 | 8.1 | Model 1 | 5.2 | Model 2 | 2.5 | Model 12 | 2.1 | Model 8 | 2.8 | Model 8 | 5.8 | COSMO | 8.6 | Model 12 | 2.3 | Model 5 | 1.4 | Model 10 | 7.9 | Model 8 | 1.7 |
| Model 1 | 3.8 | Model 2 | 11.0 | Model 9 | 5.2 | Model 7 | 2.7 | Model 10 | 2.1 | Model 5 | 2.8 | Model 1 | 5.8 | Model 6 | 8.9 | Model 6 | 2.3 | Model 8 | 1.5 | Model 5 | 8.1 | Model 5 | 2.1 |
| Model 8 | 3.8 | Model 10 | 11.0 | Model 13 | 6.0 | Model 9 | 2.8 | Model 3 | 2.7 | Model 9 | 2.8 | Model 9 | 5.8 | Model 12 | 9.6 | Model 13 | 2.4 | Model 1 | 1.5 | Model 7 | 8.3 | Model 7 | 2.4 |
| Model 2 | 5.5 | COSMO | 11.2 | COSMO | 6.6 | Model 1 | 2.8 | Model 13 | 2.7 | Model 1 | 2.8 | Model 4 | 5.9 | Model 13 | 10.1 | Model 9 | 2.4 | Model 9 | 1.5 | Model 8 | 8.4 | Model 2 | 3.3 |
| SARAH | 5.7 | SARAH | 11.5 | Model 7 | 6.7 | Model 8 | 2.8 | CMSAF | 2.9 | Model 12 | 2.9 | COSMO | 6.0 | Model 2 | 10.7 | Model 1 | 2.4 | Model 13 | 1.6 | Model 1 | 8.4 | Model 10 | 3.6 |
| Model 10 | 6.8 | Model 5 | 11.6 | Model 12 | 7.4 | Model 10 | 2.9 | Model 2 | 3.7 | Model 4 | 3.0 | Model 2 | 6.0 | Model 9 | 11.2 | Model 8 | 2.5 | Model 2 | 2.1 | Model 9 | 8.4 | Model 13 | 7.7 |
| COSMO | 6.9 | Model 8 | 12.1 | Model 3 | 7.7 | Model 5 | 3.1 | Model 9 | 4.4 | Model 10 | 3.7 | Model 13 | 6.2 | Model 1 | 11.2 | Model 2 | 2.5 | Model 14 | 3.6 | Model 2 | 8.8 | SARAH | 8.0 |
| Model 13 | 10.5 | Model 1 | 12.1 | Model 14 | 8.1 | Model 14 | 3.7 | Model 1 | 4.4 | Model 7 | 3.9 | Model 14 | 6.2 | Model 8 | 11.2 | Model 5 | 2.5 | Model 6 | 4.2 | Model 4 | 9.5 | COSMO | 8.3 |
| ERA5 | 10.6 | Model 9 | 12.1 | Model 4 | 8.5 | Model 3 | 4.2 | Model 8 | 4.4 | Model 11 | 4.2 | Model 12 | 6.3 | Model 5 | 11.3 | Model 3 | 3.5 | Model 3 | 5.1 | Model 11 | 10.4 | Model 6 | 9.0 |
| Model 6 | 11.0 | Model 11 | 14.6 | Model 10 | 10.0 | Model 11 | 4.3 | Model 5 | 4.5 | ERA5 | 4.6 | Model 6 | 6.9 | Model 7 | 12.1 | COSMO | 4.7 | CMSAF | 5.6 | Model 6 | 10.4 | Model 12 | 10.2 |
| Model 4 | 13.3 | Model 7 | 15.4 | SARAH | 10.4 | Model 4 | 6.9 | COSMO | 4.6 | SARAH | 4.8 | CMSAF | 7.1 | Model 3 | 16.8 | ERA5 | 9.1 | COSMO | 7.2 | Model 3 | 13.4 | ERA5 | 12.6 |
| Model 12 | 13.6 | CMSAF | 15.5 | CMSAF | 11.8 | SARAH | 7.3 | ERA5 | 4.7 | CMSAF | 5.1 | Model 10 | 7.4 | ERA5 | 20.7 | CMSAF | 9.9 | SARAH | 7.3 | CMSAF | 18.3 | Model 14 | 12.6 |
| Model 14 | 14.7 | Model 3 | 15.9 | Model 11 | 12.4 | CMSAF | 8.8 | Model 7 | 5.7 | COSMO | 6.0 | SARAH | 7.5 | CMSAF | 22.5 | SARAH | 10.5 | ERA5 | 7.9 | PSARAH | 20.8 | Model 4 | 13.9 |
| Model 3 | 39.1 | ERA5 | 29.8 | ERA5 | 22.3 | ERA5 | 12.7 | Model 4 | 5.7 | Model 3 | 6.7 | Model 11 | 8.7 | SARAH | 23.8 | Model 4 | 11.1 | Model 4 | 14.4 | ERA5 | 22.2 | Model 3 | 39.9 |

Green: 0-1, Pink: 1-2, Yellow: 2-3, Blue: 3-4, Orange: 4-5, White: >5

### Table 7. Statistical analysis results of the models

| Coefficients | $c_1$ | $c_2$ | $c_3$ | $c_4$ | MPE | MBE | RMSE | t | $R^2$ |
|---|---|---|---|---|---|---|---|---|---|
| Model 1 | 0.31126 | 0.38816 | | | 1.62779 | 0.10137 | 1.00516 | 0.33620 | 0.98024 |
| Model 2 | 0.00000 | 0.68273 | 0.43034 | | 1.36944 | 0.08958 | 0.97292 | 0.30667 | 0.98124 |
| Model 3 | 0.01045 | | | | -7.79935 | -0.59046 | 1.77903 | 1.16693 | 0.98415 |
| Model 4 | 0.96995 | 0.97005 | 0.00567 | | -2.78882 | -0.20903 | 1.23947 | 0.56747 | 0.97273 |
| Model 5 | 0.30655 | 0.39462 | 0.00000 | 0.35823 | 1.78399 | 0.10943 | 1.00122 | 0.36470 | 0.98066 |
| Model 6 | 1.18460 | 0.55350 | 1.31525 | | 0.52424 | 0.04773 | 0.92664 | 0.17107 | 0.98226 |
| Model 7 | 0.39025 | 0.03689 | | | 2.42743 | 0.14110 | 1.11295 | 0.42390 | 0.97692 |
| Model 8 | 0.23093 | 0.00670 | 0.00207 | 0.12927 | 1.62517 | 0.10122 | 1.00516 | 0.33571 | 0.98023 |
| Model 9 | 0.31127 | 0.00000 | 0.38815 | | 1.62798 | 0.10139 | 1.00516 | 0.33627 | 0.98024 |
| Model 10 | 0.15871 | 0 | | | 1.6279829 | 0.101392 | 1.005157 | 0.369948 | 0.981095 |
| Model 11 | 0.223418 | 0 | | | 2.6266197 | 0.174522 | 1.09458 | 0.535662 | 0.97947 |
| Model 12 | 0.91289 | 0.276647 | 0.27664727 | | -0.265234 | 0.002701 | 0.952089 | 0.009408 | 0.980939 |
| Model 13 | 0.646266 | 3.124511 | 0.175862928 | 0.161353 | 0.422136 | 0.040554 | 0.939589 | 0.143285 | 0.98166 |
| Model 14 | 0.89387 | 0.015035 | 0.196824754 | 0.031273 | -1.079894 | -0.05033 | 0.90058 | 0.185628 | 0.983274 |
| COSMO | | | | | -1.196348 | -0.25105 | 1.053134 | 0.8141 | 0.979036 |
| ERA5 | | | | | 13.438342 | 1.809879 | 2.077154 | 5.889214 | 0.978999 |
| SARAH | | | | | 8.9986237 | 1.415286 | 1.893419 | 3.731965 | 0.976245 |
| CMSAF | | | | | 8.793807 | 1.411759 | 1.840986 | 3.962675 | 0.980089 |

## 4. Conclusions

In this study, the success of empirical models and satellite-based data sets in global solar radiation estimations of Usak province were compared. In addition, 2 different models were developed and tested within the scope of this study.

According to the monthly evaluation of the models, it had absolute relative error values below 5% in March-April-May-June, September-October and December, and accurate estimates were obtained in these months. Especially in the late spring-early summer and autumn period, estimates close to the measurements were obtained. Absolute relative error below 5% was seen in May in 16 of the 18 models used. The closest estimates were made in May. The determination coefficients of empirical models and satellite-based data sets were calculated over 0.97. This result shows that the models and satellite-based data sets used are generally successful. When the success of the models within themselves was evaluated according to the RMSE values, the most successful estimations were obtained from the Model 14 data (0.90058 RMSE, 0.98327 $R^2$, -1.079894 MPE, -0.05033 MBE ve 0.185628 t), which was developed logarithmically based on the clock angle and the maximum temperature difference, using 4 constant coefficients ($c_1$, $c_2$, $c_3$ and $c_4$) from the empirical models. From the spatial data, the most successful estimates were obtained from the COSMO re-analysis data (1.053134 RMSE, 0.979036 $R^2$, -1.196348 MPE, -0.25105 MBE ve 0.8141 t). Results from satellite-based datasets (PVGIS) were not as successful as estimations made by empirical models. However, the advantage of these data was that they present ready data for wide geographies, although they were not highly sensitive. These data can be used to see the spatial radiation values of the areas to be studied or were of a nature to shed light on more superficial studies.

As a result, it had been observed that empirical models can be preferred in detailed sensitive studies for global solar radiation estimation in Usak, and satellite-based data sets (PVGIS) can be used in more superficial or pre-feasibility studies. It was concluded that Model 14 from the models and COSMO re-analysis data among satellite-based data sets (PVGIS) can be used in global solar radiation estimation studies in Usak.

| | Nomenclature | | |
|---|---|---|---|
| ARE | Absolute Relative Error | $c_n$ | $n$th coefficient |
| CAMS | Copernicus Atmosphere Monitoring Service | $G_{sc}$ | Solar constant 1367 W m$^{-2}$ |
| | | h | hour |
| CMSAF | Satellite Application Facility on Climate Monitoring | H | Average daily solar radiation on a horizontal surface (J m$^{-2}$ day$^{-1}$) |
| COSMO | Concertium for Small-Scale Modelling | $H_0$ | Monthly average daily extraterrestrial radiation on a horizontal surface |
| DHI | Diffuse radiation on a horizontal surface | $H_{io}$ | Measured H value |
| | | $H_{ip}$ | Estimated H value |
| DirHor | Direct horizontal | $i$ | ith day of month |
| ERA5 | ECMWF Reanalysis v5 | kWh | Kilowatt hour |
| GHGs | Greenhouse gases | MJ | Mega joule |
| GHI | Global radiation on a horizontal surface | n | The number of the day of the year starting from the first of January |
| GIS | Geographical Information System | $R^2$ | Determinasyon katsayısı |
| | | S | Sunshine length (h) |
| MBE | Mean Bias Error | $S_0$ | Day length (h) |
| MPE | Mean Percentage Error | t | t statistik |
| MRM | Meteorological Radiation Model | $w_s$ | Hour angle |
| | | $\pi$ | Pi |
| PVGIS | PhotoVoltaic Geographical Information System | $\Delta T$ | The difference of temperature between maximum and minimum |
| RMSE | Root Mean Square Error | $\varphi$ | Latitude |
| RS | Remote Sensing | $\delta$ | The Solar declination angle |
| SARAH | Surface Solar Radiation Data Set-Heliosat | | |
| UTM | Universal Transversal Mercator | | |

### Ethical Statement

There is no need to obtain permission from the ethics committee for this study.

### Conflicts of Interest

We declare that there is no conflict of interest between us as the article authors.

### Authorship Contribution Statement

Concept: Ersan, R. Külcü, R.; Design: Ersan, R. Külcü, R.; Data Collection or Processing: Ersan, R.; Statistical Analyses: Ersan, R.; Literature Search: Ersan, R.; Writing, Review and Editing: Ersan, R. Külcü, R.

# References

Almorox, J. and Hontoria, C. (2004). Global solar radiation estimation using sunshine duration in Spain. *Energy Conversion and Management*, 45: 1529–35.

Almorox, J., Bocco, M. and Willington, E. (2013). Estimation of daily global solar radiation from measured temperatures at Cañada de Luque, Córdoba, Argentina. *Renewable Energy*, 60: 382-387.

Ampratwum, D. B. and Dorvlo, A. S. S. (1999). Estimation of solar radiation from the number of sunshine hours. *Applied Energy*, 63: 161–7.

Anacan, R. M., Cabautan, A. C., Cayabyab, J. M. A., Miguel, S. X. A., Modrigo, V. D., Rosites, C. J. V. and Sagun, A. C. (2018). Development of oil quality estimator using machine vision system. *In 2018 IEEE 10th International Conference on Humanoid, Nanotechnology, Information Technology, Communication and Control, Environment and Management (HNICEM)* 29 November - 02 December, P. 1-6, Baguio City, Philippines.

Angstrom, A. (1924). Solar and terrestrial radiation. Report to the international commission for solar research on actinometric investigations of solar and atmospheric radiation. *Quarterly Journal of the Royal Meteorological Society,* 50(210): 121-126.

Anonymous (2020a). Pre-Investment feasibility of electricity generation from solar energy in Usak industry. https://investinusak.gov.tr/assets/upload/dosyalar/usak-sanayisinde-gunes-enerjisinden-elektrik-uretiminin-yatirim-oncesi-fizibilitesi.pdf/ (Accessed Date: 24.04.2020).

Anonymous (2020b). Land use of Usak province. Prime Ministry, Republic of Turkey, General Directorate of Rural Services Publications, Report No: 64, Ankara, Turkey.

Anonymous (2020c). Climate data of Usak for long years. https://www.mgm.gov.tr/veridegerlendirme/il-ve-ilceler-istatistik.aspx?m=USAK/ (Accessed Date: 17.12.2020).

Anonymous (2021a). Solar energy map of Usak province, https://www.enerjiatlasi.com/gunes-enerjisi-haritasi/usak/ (Accessed Date: 04.01.2021).

Anonymous (2021b). PVGIS users manuel. https://ec.europa.eu/jrc/en/PVGIS/docs/usermanual/ (Accessed Date: 09.01.2021).

Anonymous (2021c). Numerical Analysis. https://web.karabuk.edu.tr/yasinortakci/dokumanlar/say%C4%B1sal_analiz/turkce/2.pdf/ (Accessed Date: 01.03.2021).

Artkın, F. (2018). The renewable energy sources and technologies of potential in Turkey. *The Eurasia Proceedings of Science Technology Engineering and Mathematics*, 4: 285-295.

Bahel, V., Bakhsh, H. and Srinivasan, R. (1987). A correlation for estimation of global solar radiation. *Energy*, 12: 131–5.

Bristow, K. L. and Campbell, G. (1984). On the relationship between incoming solar radiation and daily maximum and minimum temperature. *Agricultural and Forest Meteorology,* 31(2): 159-166.

Cooper, P. I. (1969). The absorption of solar radiation in solar stills. *Solar Energy*, 12: 3.

Coppolino, S. (1994). A new correlation between clearness index and relative sunshine. *Renewable Energy*, 4(4): 417-423.

Dogniaux, R. and Lemoine, M. (1983). Classification of radiation sites in terms of different indices of atmospheric transparency. *Solar energy research and development in the European Community, Dordrecht, Holland: Reidel,* Series F, Dordrecht, Holland: Reidel; 2:94–107.

Duffie, J. A. and Beckman, W. A. (1980). Solar Engineering of Thermal Processes. 4th Edition, Wiley, New York, U.S.A.

Dyer, S. A. and Dyer, J. S. (2007). Approximations to error functions. *IEEE Instrumentation & Measurement Magazine*, 10(6): 45-48.

Elagib, N. and Mansell, M. (2000). New approaches for estimating global solar radiation across Sudan. *Energy Conversion and Management*, 41(5): 419-434.

El-Metwally, M. (2005). Sunshine and global solar radiation estimation at different sites in Egypt. *Journal of Atmospheric and Solar-Terrestrial Physics*, 67(14): 1331–1342.

Feng, Y., Chen, D. and Zhao, X. (2019). Improved empirical models for estimating surface direct and diffuse solar radiation at monthly and daily level: A case study in North China. *Progress in Physical Geography: Earth and Environment,* 43(1): 80-94.

Frank, C. W., Wahl, S., Keller, J. D., Pospichal, B., Hense, A. and Crewell, S. (2018). Bias correction of a novel European reanalysis data set for solar energy applications. *Solar Energy*, 164: 12–24.

Green, K. and Tashman, L. (2009). Percentage error: What denominator?. *Foresight: The International Journal of Applied Forecasting, , International Institute of Forecasters* 12: 36-40.

Güçlü, Y. S. (2019). Hybrid model for solar irradiation estimation using polynomial and Angström-Prescott equation. *Selcuk University Journal of Engineering, Science and Technology*, 7(1): 75-88 (In Turkish).

Gül, M. and Çelik, E. (2017). Global solar radiation estimation for Tunceli province using ANFIS. *Dicle University Faculty of Engineering, Engineering Journal*, 8(4): 891-899 (In Turkish).

Hargreaves, G. L., Hargreaves, G. H. and Riley, J. P. (1985). Irrigation water requirements for Senegal River basin. *Journal of Irrigation and*

*Drainage Engineering*, 111(3): 265-275.

Ineichen, P. (2014). Long term satellite global, beam and diffuse irradiance validation. *Energy Procedia*, 48: 1586–1596.

Işık, E. and İnallı, M. (2011). Global radiation predict by using artificial neural network for Tunceli city. *Journal of New World Sciences Academy, Engineering Sciences,* 6(1): 190-194.

Kallioğlu, M. A., Karakaya, H. and Avci, A. S. (2015). Analysis of sunshine hours and global solar radiation for Mardin of Turkey. *3rd International Symposium on Innovative Technologies in Engineering and Science*, *Universitat Politecnica de Valencia*, 3-5 June, Valencia, Spain.

Kimball, H. H. (1919). Variations in the total and luminous solar radiation with geographical position in the United States. *Monthly Weather Review*, 47(11), 769-793.

Klein, S. A. (1977). Calculation of monthly average insolation on tilted surfaces. *Solar Energy*, 19: 325.

Kulcu, R., Suslu, A., Cihanalp, C. and Yilmaz, D. (2017). Modelling of global solar radiation on horizontal surfaces for Mersin city. *Wind Energy*, 433(216): 127-4.

Külcü R. (2015). Modelling of solar radiation reaching the earth to Isparta province. Süleyman Demirel University, *Journal of The Faculty of Agriculture*, 10(1): 19-26.

Külcü R. (2019). Development of a new model using empirical modeling of global solar radiation and its application in Çankırı city. *Yekarum*, 4(2): 1-8 (In Turkish).

Külcü, R. and Ersan, R. (2021). Empirical modelling of global solar radiation in Hatay (Turkey) province. *Journal of Tekirdag Agricultural Faculty*, 18(3): 446 - 456 (In Turkish).

Marfo, P. and Okyere, G. A. (2019). The accuracy of effect-size estimates under normals and contaminated normals in meta-analysis. *Heliyon*, 5(6): e01838.

Navarro M. C. (1992). *Small area estimation: estimating selected economic statistics for provinces of the Philippines.* (MSc. Thesis) Statistics, Australian National University, Canberra, Australia.

Önler, E. and Kayışoğlu, B. (2023). Estimation of monthly, seasonal and annual total solar radiation on the tilted surface at optimum tilt angles in two provinces, Turkiye. *Journal of Tekirdag Agricultural Faculty*, 20(3): 712-722.

Prescott J. (1940). Evaporation from a water surface in relation to solar radiation. *Transactions of the Royal Society of South Australia*. 64(1): 114-118.

Psiloglou, B. E., Kambezidis, H. D., Kaskaoutis, D. G., Karagiannis, D. and Polo, J. M. (2020). Comparison between MRM simulations, CAMS and PVGIS databases with measured solar radiation components at the Methoni station, Greece. *Renewable energy,* 146: 1372-1391.

Skeiker, K. (2006). Correlation of global solar radiation with common geographical and meteorological parameters for Damascus province, Syria. *Energy Conversion and Management*, 47(4): 331-345.

Supit, I. and Van Kappel, R. R. (1998). A simple method to estimate global radiation. *Solar Energy*, 63(3): 147-160.

Tırmıkçı, C.A. (2018). *Real time comparison of a two axis solar tracking system and an optimally tilted fixed solar System for yearly adjustment*. (Ph.D. Thesis) Sakarya University, Institute of Natural Sciences, Electrical and Electronics Engineering Department, Sakarya, Turkey.

Urraca, R., Gracia-Amillo, A. M., Huld, T., Martinez-de-Pison, F. J., Trentmann, J., Lindfors, A. V., Riihela, A and Sanz-Garcia, A. (2017). Quality control of global solar radiation data with satellite-based products. *Solar Energy*, 158: 49-62.

Urraca, R., Huld, T., Gracia-Amillo, A., Martinez-de-Pison, F. J., Kaspar, F. and Sanz-Garcia, A. (2018). Evaluation of global horizontal irradiance estimates from ERA5 and COSMO-REA6 reanalyses using ground and satellite-based data. *Solar Energy*, 164: 339–354.